Nonlinear propagation of short intense laser pulses in a hollow metallic waveguide

N. E. Andreev,[1] C. Courtois,[2] B. Cros,[2] L. M. Gorbunov,[3] and G. Matthieussent[2]
[1]*Institute for High Energy Densities, Associated Institute for High Temperatures of RAS, Izhorskaya 13/19, Moscow 127412, Russia*
[2]*LPGP, UMR 8578, CNRS, Université Paris XI, Batiment 210, 91405 Orsay, France*
[3]*Lebedev Physics Institute of RAS, Leninskii prospekt 53, Moscow 117924, Russia*
(Received 4 December 2000; published 19 June 2001)

The propagation of a short intense laser pulse in the femtosecond range in a hollow metallic waveguide gives rise to heating of the metallic wall. The temperature of the degenerate electron gas in the wall is increased during the pulse duration and this heating affects the propagation and dissipation of the laser pulse. Analytical and numerical analysis shows that, as the dissipation is increased, the leading edge of the pulse decreases more slowly than the rear, resulting in a pulse shortening.

DOI: 10.1103/PhysRevE.64.016404 PACS number(s): 52.38.−r

I. INTRODUCTION

Recent progress in the generation of ultraintense short laser pulses (see, for example, Ref. [1]) has made possible a number of scientific and technical applications, such as plasma-based particle accelerators [2], x-ray lasers [3], inertial confinement fusion [4], and laser induced nuclear reactions [5]. The propagation of a pulse over a long distance is a crucial condition for all these applications. However, the length of the high intensity laser region is typically limited by the laser diffraction, which is twice the Rayleigh length. Various methods are now being investigated to overcome this limitation. One of them is based on the relativistic and ponderomotive self-channeling of pulses in a plasma [6]. Another method is to guide a laser pulse in a preformed plasma density channel [7] produced as a result of gas ionization by another laser pulse [8] or by slow capillary discharge [9]. An alternative approach is the use of solid guides, namely, capillary tubes.

The transmission of laser pulses up to 1 TW through hollow glass capillary tubes with diameters of the order of 100 μm was studied first in [10] and for laser pulses with power 10 TW in [11]. In both of these experiments the guiding was multimode, leading to a complex transverse intensity repartition of the transmitted light. Monomode guiding in hollow capillary dielectric tubes of intense laser pulses (10^{16} W/cm^2) over 100 Rayleigh lengths was demonstrated in [12]. Experiments with higher pulse intensities in metallic and dielectric hollow tubes as well as with gas filled tubes are now in progress.

Within the usual linear theory, the propagation of electromagnetic waves in a capillary tube is supposed to be independent of the wave intensity (see, for example, [13]). This approximation becomes invalid for high intensity laser pulses, as the properties of the tube walls and of the filling gas are modified by the laser pulse. In the case of sufficiently low gas pressure the nonlinear effects arising because of gas ionization and walls heating may be treated as independent.

The aim of this paper is to formulate the basic equations describing self-consistently the short intense laser pulse propagation and wall heating in the case of a hollow metallic waveguide. For simplicity, the propagation of the laser pulse will be considered in a plane waveguide. The electron temperature in the walls is assumed to remain less than the Fermi temperature. In addition the pulse duration is taken to be so small that the ions of the metal lattice may be considered as immobile.

The analytical and numerical solutions of the basic equations show that the trailing part of a laser pulse dissipates more than the leading one. As a result of this nonlinear effect the form of the propagating pulse is changed so that the pulse duration decreases and the overall pulse attenuation increases. Naturally, the nonlinear effects become weaker in the process of pulse propagation as its intensity decreases.

II. BASIC EQUATIONS

To investigate the problem of the nonlinear effects due to heating of waveguide walls on short laser pulse propagation we study here for simplicity the slab geometry. Let us consider a waveguide with metallic walls at $|y| \geqslant a$ and with axis along *OZ*, the direction of propagation.

The electric field of the laser pulse is taken in the form

$$\tilde{\mathbf{E}} = \mathrm{Re}\{\mathbf{E}\exp(-i\omega t + ikz)\},$$

where ω and k are the frequency and the axial component of the wave vector of the laser radiation, respectively, and $\mathbf{E}(y,z,t)$ is the slowly varying (on the scales $1/\omega$ and $1/k$) complex amplitude of the field. For the pulse envelope $\mathbf{E}(y,z,t)$ we have from Maxwell's equations

$$2i\omega\left(\frac{\partial}{\partial t} + V_g\frac{\partial}{\partial z}\right)\mathbf{E} + c^2\frac{\partial^2\mathbf{E}}{\partial y^2} + (\omega^2\epsilon - k^2c^2)\mathbf{E} = \mathbf{0}, \quad (1)$$

where $V_g = kc^2/\omega$ is the group velocity and ϵ is the dielectric constant, assumed to be equal to unity in the vacuum part of the waveguide ($|y| < a$). The effect of group velocity dispersion is omitted, assuming that the nonlinear effect of the wall heating is more important for the evolution of the laser pulse envelope. Thus small corrections due to dispersion of the dielectric function of the walls ϵ, its space and time derivatives, and higher order derivatives of the electric field envelope are omitted in this equation.

Multiplying Eq. (1) by the complex conjugate amplitude $\mathbf{E}^*$ and integrating over y from $-\infty$ to $+\infty$ we arrive at the

following equation for the electromagnetic energy variation in each cross section of the laser pulse propagating in the waveguide:

$$\left(\frac{\partial}{\partial t}+V_g\frac{\partial}{\partial z}\right)\int_{-a}^{a}\frac{|\mathbf{E}|^2}{8\pi}dy=-\frac{\omega}{4\pi}\int_{a}^{\infty}\mathrm{Im}(\epsilon)|\mathbf{E}|^2\,dy, \quad (2)$$

where symmetry of the field $|\mathbf{E}(-y)|=|\mathbf{E}(y)|$ was assumed and the small value of the energy in the skin layers of the walls was neglected in comparison with the energy in the vacuum part of the waveguide.

The transverse structure of the waveguide modes is determined by Eq. (1) and by the boundary conditions corresponding to the continuity of the tangential components of the electric and magnetic fields at the wall surfaces $y=\pm a$. The explicit analytical form of the mode structure can be found if the spatial variation of the dielectric constant ϵ (due to heating of the walls by the laser pulse) is small on the scale of the skin depth. This is just the case of the high frequency skin effect (see, e.g., [14]) when the real part of the dielectric constant (which determines the field structure) remains constant while the small imaginary part [$\mathrm{Im}\,\epsilon \ll |\epsilon|$] responsible for the laser pulse absorption can be changed substantially due to the heating of the waveguide walls during the laser pulse propagation. The physical conditions for this regime will be discussed later. With these restrictions in mind, let us specify the energy conservation law (2) for different waveguide modes.

A. *S*-polarized laser field (TE modes)

In this case the electric field $\mathbf{E}=(E_x,0,0)$ has an x component only and a solution of Eq. (1) can be found in the form

$$E_x=E_0(z-V_g t,z)Y_n(y), \quad (3)$$

where for symmetrical modes

$$Y_n(y)=\begin{cases}\cos(k_\perp^{(n)}y), & |y|<a\\ b\,\exp[-\kappa(|y|-a)] & |y|>a,\end{cases} \quad (4)$$

$\kappa\cong\sqrt{k^2-(\omega^2/c^2)\epsilon}$ in accordance with Eq. (1), and $\mathrm{Re}\,\kappa>0$, while $\mathrm{Re}\,\epsilon<0$ for metallic walls. The continuity of E_x and $\partial E_x/\partial y\propto B_z$ at the waveguide walls $y=\pm a$,

$$b=\cos(k_\perp^{(n)}a), \quad (5)$$

$$\kappa b=k_\perp^{(n)}\sin(k_\perp^{(n)}a),$$

determines the boundary field amplitude at the wall b and the dispersion equation for the transverse wave vector $k_\perp^{(n)}$:

$$\tan(k_\perp^{(n)}a)=\frac{\kappa}{k_\perp^{(n)}}. \quad (6)$$

For wide enough waveguides (in comparison with the laser wavelength $\lambda=2\pi c/\omega \ll a$) and for modes with not very high numbers n, when $|\kappa|\gg k_\perp^{(n)}$, the solutions to Eq. (6) are

$$k_\perp^{(n)}\cong\frac{\pi}{2a}\left(1-\frac{1}{\kappa a}\right)(1+2n), \quad n=0,1,2,\ldots. \quad (7)$$

This expression together with Eqs. (3)–(5) gives the following ratio of the laser field at the wall E_w to the field on the waveguide axis E_0:

$$\left|\frac{E_w}{E_0}\right|\equiv b\cong\frac{\pi}{2}\frac{(1+2n)}{|\kappa|a}. \quad (8)$$

For each mode (4), Eqs. (3) and (8) enable one to write down the equation for the electromagnetic energy variation (2) in the form

$$\frac{\partial}{\partial z}\ln|E_0(\xi,z)|^2=-2\frac{\omega}{V_g a}\left|\frac{E_w}{E_0}\right|^2\int_a^\infty \mathrm{Im}(\epsilon)\times\exp[-2\,\mathrm{Re}(\kappa)(y-a)]dy, \quad (9)$$

where we introduced the new variables z and $\xi=z-V_g t$, which determine the distance of the laser pulse propagation and the form of the pulse envelope in the comoving frame. The group velocities of distinct modes are different, but, in accordance with Eq. (1), for not very high mode numbers they are close to the speed of light:

$$V_g\equiv\frac{kc^2}{\omega}\cong c\left[1-\frac{(1+2n)^2}{32}\left(\frac{\lambda}{a}\right)^2\right]. \quad (10)$$

It is worth noting also that in a linear regime, when $\mathrm{Im}\,\epsilon=\mathrm{Im}\,\epsilon_0=\mathrm{const}$, Eq. (9) takes the form

$$\frac{\partial}{\partial z}\ln|E_0(\xi,z)|^2=-2k_0''\equiv-\frac{\omega}{V_g\,\mathrm{Re}(\kappa)a}\left|\frac{E_w}{E_0}\right|^2\mathrm{Im}\,\epsilon_0, \quad (11)$$

which can be obtained directly from Eq. (1) by introducing $E_0(\xi,z)=\overline{E_0}(\xi)\exp(-k_0''z)$ in Eq. (3). The imaginary part of the longitudinal wave vector k_0'' is determined by the dispersion equation, which follows from Eq. (1), through the imaginary part of $k_\perp^{(n)}$ specified by Eq. (6). Therefore it is given by

$$k_0''=\frac{\pi^2}{8}\frac{(1+2n)^2}{\mathrm{Re}(\kappa)|\kappa|^2a^3}\frac{\omega}{V_g}\mathrm{Im}\,\epsilon_0$$

in full agreement with Eqs. (8) and (11).

B. *P*-polarized laser field (TM modes)

In this case the laser pulse has only an x component for the magnetic field B_x and two components of the electric field

$$E_y\cong-\frac{B_x}{\epsilon}, \quad E_z\cong-i\frac{c}{\omega\epsilon}\frac{\partial B_x}{\partial y}. \quad (12)$$

Let us use for the y component of the electric field a form analogous to Eq. (3):

$$E_y = E_0(z - V_g t, z) Y_n(y), \tag{13}$$

where the transverse structure of the modes is determined by Eq. (4). The continuity of tangential components E_z and B_x at the waveguide walls $y = \pm a$, which corresponds in accordance with Eq. (12) to the continuity of $\partial E_y/\partial y$ and ϵE_y, leads to the following boundary conditions:

$$\epsilon b = \cos(k_\perp^{(n)} a), \tag{14a}$$

$$\kappa b = k_\perp^{(n)} \sin(k_\perp^{(n)} a), \tag{14b}$$

and to the dispersion equation for the transverse wave vector $k_\perp^{(n)}$

$$\tan(k_\perp^{(n)} a) = \frac{\kappa}{\epsilon k_\perp^{(n)}}. \tag{15}$$

Under the condition $|k_\perp^{(n)}| \ll |\kappa/\epsilon|$ [i.e., $(1+n)\lambda/a \ll 4/|\epsilon|^{1/2}$], the solutions of this equation are

$$k_\perp^{(n)} \cong \frac{\pi}{2a}\left(1 - \frac{\epsilon}{\kappa a}\right)(1+2n), \quad n = 0,1,2, \ldots . \tag{16}$$

Due to Eqs. (12), the longitudinal component E_z is proportional to the transverse derivative of E_y:

$$E_z \cong i \frac{c}{\omega} \frac{\partial E_y}{\partial y}. \tag{17}$$

It is evident from Eqs. (13), (4), and (16) that, inside the waveguide ($|y| < a$), the amplitude of E_z is small in comparison with E_y (as $|k_\perp^{(n)}|\lambda \ll 1$), while in the walls ($|y| > a$) the inverse ratio is valid: $|E_z/E_y|^2 \cong |\epsilon| \gg 1$. This means that, in the left hand side of the conservation law (2), only the transverse component E_y has to be taken into account, while in the right hand side of Eq. (2) the main component of the laser field is the longitudinal one E_z. Equations (17) and (13) together with (14) and (16) determine the ratio of the z component of the laser field at the wall $E_z(y=a) \equiv E_w$ to the y component field on the waveguide axis $E_y(y=0) \equiv E_0$:

$$\left|\frac{E_w}{E_0}\right| \cong \frac{\pi}{2} \frac{(1+2n)}{a\omega/c}. \tag{18}$$

As a result, for each TM mode the equation for electromagnetic energy variation (2) has exactly the same form (9) as for TE modes, but in the case of a *P*-polarized laser field the ratio $|E_w/E_0|^2$ is determined by Eq. (18). The group velocities of TM modes are determined as before by Eq. (10) if the mode number is not very high: $1 + 2n \ll 4a/(\lambda|\epsilon|^{1/2})$. For the propagation of the TM mode in a linear regime, when $\mathrm{Im}\,\epsilon = \mathrm{Im}\,\epsilon_0 = \mathrm{const}$, Eq. (9) takes the form (11) which again can be obtained directly from Eq. (1) with $E_0(\xi, z) = \overline{E_0}(\xi)\exp(-k_0'' z)$ in Eq. (13). Therefore the imaginary part of the longitudinal wave vector is given by

$$k_0'' = \frac{\pi^2}{8} \frac{(1+2n)^2}{\mathrm{Re}(\kappa)(\omega/c)^2 a^3} \frac{\omega}{V_g} \mathrm{Im}\,\epsilon_0,$$

in full agreement with Eqs. (11) and (18).

Equations (8), (18), and (9) show that the attenuation of TM modes due to absorption in the metallic walls is much higher, by a factor of $|\epsilon| \gg 1$, than that of TE modes with the same mode number *n*. The absorption increases strongly for higher mode numbers as $(1+2n)^2$, and decreases for wider waveguides as a^{-3}. These equations, providing $\mathrm{Im}\,\epsilon$ is known, describe the laser pulse propagation in an absorbing metallic waveguide with regard to a nonlinear modification of the pulse's temporal shape due to the heating of the walls by laser radiation.

C. Model of metallic walls

To describe the high frequency response of the metallic walls we use the Drude-Sommerfeld model for the dielectric constant of metals [15,16]:

$$\epsilon = 1 - \frac{\omega_p^2}{\omega(\omega + i\nu)}, \tag{19}$$

where ω_p and ν are the plasma and collision frequencies of electrons, respectively. For laser wavelengths of the order of 1 μm, the inequality $\omega_p \gg \omega$ is valid; the electron collision frequency has to be small compared to the laser frequency ($\nu \ll \omega$). These conditions correspond to the high frequency skin effect [14] when the real and imaginary parts of the dielectric constant are given by

$$\mathrm{Re}\,\epsilon \cong -\frac{\omega_p^2}{\omega^2}, \quad \mathrm{Im}\,\epsilon \cong \frac{\omega_p^2}{\omega^2}\frac{\nu}{\omega}. \tag{20}$$

The energy of a short, subpicosecond laser pulse, is transferred mainly to electrons while the change in the lattice temperature T_{lat} is relatively small. Therefore the electron thermal energy is determined mainly by the processes of laser heating and electron heat conduction:

$$C\frac{\partial T_e}{\partial t} - \frac{\partial}{\partial y}\left(\kappa_T \frac{\partial T_e}{\partial y}\right) = \frac{\omega}{8\pi}\mathrm{Im}(\epsilon)|\mathbf{E}|^2, \tag{21}$$

where T_e is the electron temperature; C the thermal capacity and κ_T the thermal conductivity in the case of a degenerate electron gas ($T_e < T_F$) have the forms

$$C(T_e) = \frac{\pi^2}{2} n_e \frac{T_e}{T_F}, \quad \kappa_T(T_e) = \frac{1}{3} V_F^2 \frac{C(T_e)}{\nu(T_e)}. \tag{22}$$

T_F and V_F are the Fermi temperature and velocity, respectively, and n_e is the density of conduction electrons.

For sufficiently low intensities of the laser radiation at the walls, when the electron temperature T_e does not exceed the Fermi temperature T_F, the plasma frequency ω_p can be assumed to be a constant and the temperature dependence of the electron collision frequency has the form [17]

$$\nu(T_e) = \nu_0\left[1 + \frac{T_e^2}{T_F T_{\mathrm{lat}}}\right], \tag{23}$$

where $\nu_0 \approx T_{\rm lat}/\hbar$ is the electron-phonon collision frequency and the lattice temperature $T_{\rm lat}$ is assumed to be larger than the Debye temperature. The second term in Eq. (23) corresponds to electron-electron collisions [15,16] and becomes predominant for a sufficiently overheated electron system when $T_e > T^* = (T_{\rm lat} T_F)^{1/2} \approx 0.3\,{\rm eV}$ for typical parameters of metals ($T_F \approx 5$ eV, $T_{\rm lat} \approx 2.6\times 10^{-2}$ eV$=300$ K).

It should be noted that in Eq. (21) the collisions of electrons with the metal boundaries were omitted. This means that this assumption is correct if the skin depth $\delta \cong \kappa^{-1} \cong c/\omega_p$ is large compared to the electron mean free path $l_e \approx V_F/\nu$. Also, the concept of a temperature also supposes the smallness of l_e in comparison with the scale of temperature variations, which can be of the order of the skin depth. At room temperature the ratio (δ/l_e), calculated on the base of data taken from [15], is of the order of 0.3–0.5 for copper, near to 0.8 for aluminum, and around 4 for lead. Therefore, this assumption is acceptable for lead from room temperature, while for Cu and Al it is quantitatively correct after some preheating of electrons from room temperature to $T_e > T^*$.

As long as the electron collision frequency ν is small compared to the laser frequency, a condition that can be written as $T_e < T^* (\omega/\nu_0)^{1/2}$, the imaginary part of the dielectric constant is determined by Eqs. (20) and (23):

$$\mathrm{Im}\,\epsilon = \frac{\omega_p^2 \nu_0}{\omega^3}\left(1+\frac{T_e^2}{T_F T_{\rm lat}}\right) \equiv \mathrm{Im}(\epsilon_0)\left(1+\frac{T_e^2}{T_F T_{\rm lat}}\right). \quad (24)$$

In the frame comoving with the laser pulse and with variables $\xi = z - V_g t$ and z, which were used in Eq. (9), the heat conduction Eq. (21), in view of Eqs. (22)–(24), can be transformed for the function

$$G(\xi,y,z) = \ln Y(\xi,y,z) \equiv \ln\left(1+\frac{T_e^2}{T_F T_{\rm lat}}\right),$$

to the equation

$$\frac{\partial G}{\partial \xi} = -\beta I(\xi,z)\exp\left(-2\frac{\omega_p}{c}(y-a)\right) - D\exp(-G)\frac{\partial^2 G}{\partial y^2}. \quad (25)$$

The laser pulse intensity on the waveguide axis $I(\xi,z) = c|E_0(\xi,z)|^2/8\pi$ is determined for S or P polarization by the x or y component of the laser electric field envelope (3) or (13), respectively;

$$\beta = \frac{4}{\pi^3}\frac{r_0 \lambda^2}{c T_{\rm lat}}\frac{\nu_0}{c}\left|\frac{E_w}{E_0}\right|^2, \quad D = \frac{1}{3}\frac{V_F^2}{c\,\nu_0}, \quad (26)$$

$r_0 = e^2/mc^2$ is the classical electron radius, and $|E_w/E_0|$ is determined by Eq. (8) or Eq. (18) for TE or TM modes respectively. By means of the expression (24) the temperature dependence of the laser pulse absorption in Eq. (9) can be explicitly written through the function G:

$$\frac{\partial}{\partial z}\ln I(\xi,z) = -2k_0'' \int_a^\infty \exp\left[G(\xi,y,z) - 2\frac{\omega_p}{c}(y-a)\right]\frac{2\omega_p}{c}dy, \quad (27)$$

where $\mathrm{Re}\,\kappa$ has been taken as ω_p/c and $2k_0''$ is the linear attenuation coefficient determined by Eq. (11) and, in accordance with Eq. (24), equal to

$$2k_0'' = \frac{c}{V_g a}\left|\frac{E_w}{E_0}\right|^2 \frac{\omega_p \nu_0}{\omega^2} \quad (28)$$

Going back to the heat conduction equation (21), one can get some insight into the heating mechanism in the wall by considering the characteristic length of diffusion L_D, which is defined as

$$L_D = \left(\frac{\kappa_T \tau_p}{C}\right)^{1/2} \equiv \left(\frac{V_F^2}{3\nu}\tau_p\right)^{1/2}, \quad (29)$$

where τ_P is the laser pulse duration. The comparison of the diffusion length L_D with the skin depth $\delta \sim \kappa^{-1}$, where energy deposition occurs, leads to two different regimes for the heating of the wall. If $L_D \gg \delta$, the laser energy deposited in the skin depth diffuses from the metallic surface and the heating is dominated by thermal diffusion. If $L_D < \delta$, the thermal conduction is blocked and the energy deposition occurs in the skin depth; then one can neglect the diffusion term in the heat conduction equation and this can be done provided the following inequality is satisfied:

$$\frac{\nu_0}{\omega_p}\left(1+\frac{T_e^2}{T_F T_{\rm lat}}\right) \gg \frac{\omega_p \tau_p}{3}\frac{V_F^2}{c^2}. \quad (30)$$

This last regime gives rise to local heating: the temperature in the skin depth increases on a much shorter time scale and reaches much higher values than in the regime controlled by conduction. These effects are due to the dependence of the diffusion coefficient on the inverse square of the electron temperature as shown by Eqs. (22) and (23).

From the previous expressions for the **E** and **B** fields in the waveguide and using the Poynting vector, one can express the flux of energy that is dissipated in the wall Φ_w and the laser flux at the center of the hollow metallic wave guide Φ_c. The ratio of these two fluxes can be written for S polarization as

$$\frac{\Phi_w}{\Phi_c} = \frac{\pi^2(1+2n)^2}{8k^2a^2}\frac{\nu(T_e)}{\omega}\frac{\omega}{\omega_p}, \quad (31)$$

and for P polarization as

$$\frac{\Phi_w}{\Phi_c} = \frac{\pi^2(1+2n)^2}{8k^2a^2}\frac{\nu(T_e)}{\omega}\frac{\omega_p}{\omega}. \quad (32)$$

If the absorbed flux at the wall is greater than the flux for which plasma formation occurs at the metal wall during the

pulse duration of the laser, the model will not hold and the thermal capacity and conductivity of the plasma produced at the wall have to be taken into account together with the electron-electron collision frequency in the plasma.

Therefore, in this model of a degenerate electron gas, the set of equations (25)–(28) describes self-consistently the laser pulse propagation in a metallic waveguide with heating of waveguide walls as long as the electron temperature remains less than the Fermi temperature of the metal and as long as no ionization takes place.

III. SIMPLIFIED ANALYTICAL SOLUTION (LOCAL HEATING)

For short enough laser pulses and for metals with not too small electron collision frequencies ν_0, the heat conductivity has no significant influence on the variation of the electron temperature (the corresponding conditions will be derived later). In this case the second term in the right hand side of Eq. (25) can be neglected and the solution of Eq. (25) can be written in the form

$$G(\xi,y,z)=G_0(\xi,z)\exp\left[-2\frac{\omega_p}{c}(y-a)\right],$$

$$G_0(\xi,z)\equiv G(\xi,y=a,z)=\beta\int_{\xi}^{\infty}I(\xi',z)d\xi'. \tag{33}$$

Equation (27), which gives the shape of the laser pulse as it propagates along the waveguide, can be written as

$$\frac{\partial}{\partial z}\ln I(\xi,z)=-\frac{2k_0''}{G_0}[\exp(G_0)-1]. \tag{34}$$

In the limit $G_0\to 0$, which corresponds to the omission of nonlinear effects due to wall heating, this equation is transformed to the linear Eq. (11).

The explicit analytical solution to the set of Eqs. (29), (30) can be found for small variations of the initial laser pulse shape when $G_0<1$ and in Eq. (29) the approximation $I(\xi,z)\cong I(\xi,z=0)$ can be used. Then we have

$$I(\xi,z)=I(\xi,z=0)\times\exp\left[-2k_0''z\left(1+\frac{1}{2}\beta\int_{\xi}^{\infty}I(\xi',z=0)d\xi'\right)\right]. \tag{35}$$

To point out the nonlinear effect of the laser pulse shape deformation due to the heating of the waveguide walls, let us consider the initially rectangular laser pulse envelope

$$I(\xi,z=0)=I_0[\Theta(\xi+L)-\Theta(\xi)], \tag{36}$$

where $L=c\tau_p$ is the initial pulse length. With Eq. (32) the solution (31) takes the form

$$I(\xi,z)=I_0\exp[-2k_0''z(1+\tfrac{1}{2}\beta I_0|\xi|)],\quad -L\leqslant\xi\leqslant 0. \tag{37}$$

The solution (37) evidently shows that the leading part of the laser pulse ($\xi\to 0$) evolves as in the linear case while the rear part of the pulse dissipates more strongly due to the wall heating. This effect leads to shortening of the pulse during its propagation in the waveguide. Equation (37) can be used for a crude estimation of the pulse length decrease. For a long enough distance of propagation, the full width at half maximum duration of the pulse l_{FWHM} decreases as the inverse power of the laser intensity and of the length of propagation:

$$l_{\mathrm{FWHM}}(z)=\frac{\ln 2}{\beta I_0}\frac{1}{k_0''z},\quad k_0''z>\frac{\ln 2}{\beta I_0 L}. \tag{38}$$

As an example let us consider the laser pulse with the carrier frequency $\omega=2\times10^{15}\ \mathrm{s}^{-1}$ and duration $\tau_p=50$ fs, propagating in the form of the fundamental TM mode ($n=0$) into a metallic waveguide made of lead ($\omega_p=2.13\times10^{16}\ \mathrm{s}^{-1}$, $V_F=1.83\times10^8$ cm/s, $\nu_0=7.1\times10^{14}\ \mathrm{s}^{-1}$ [15]) with a width $2a=40\ \mu$m. The thermoconductivity term in Eq. (21) is smaller than the term related to thermocapacity due to the inequality

$$(\nu_0/\omega)>(\omega_p\tau_p/3)(V_F/c)^2.$$

which is valid for the parameters indicated above. The maximum laser intensity I_0 at the entrance of the waveguide is taken to be 10^{14} W/cm^2. Then in accordance with Eq. (38) for distances of propagation exceeding 20 cm the pulse length decreases as

$$l_{\mathrm{FWHM}}/L\approx 20/z.$$

IV. NUMERICAL RESULTS

The set of Eqs. (25)–(28), describing the evolution of the laser pulse shape and of the temperature in the wall as the pulse propagates along the waveguide, was solved numerically for the main TM mode with $n=0$ in Eq. (18). The initial temporal laser pulse envelope was taken to be Gaussian:

$$I(\xi,z=0)=I_0\exp\left[-4\ln 2\frac{\xi^2}{(c\tau_p)^2}\right], \tag{39}$$

with the FWHM pulse duration $\tau_p=100$ fs, intensity on the waveguide axis at the entrance of the capillary $I_0=3\times10^{15}$ W/cm,^{2}, and wavelength $\lambda=0.8\ \mu$m ($\omega=2.35\times10^{15}\ \mathrm{s}^{-1}$). The width of the Cu waveguide was taken as $2a=20\ \mu$m, and the other parameters were [15] $T_F=8$ eV, $\nu_0=0.4\times10^{14}\ \mathrm{s}^{-1}$, and $\omega_p=1.6\times10^{16}\ \mathrm{s}^{-1}$.

The results of the calculations are presented in Figs. 1 and 2. Figure 1 shows the normalized on-axis intensity $I_{\max}(z)/I_0$ and maximum electron temperature $T_{e,\max}/T_F$ reached on the wall as functions of the distance of laser pulse propagation. The result of the linear theory (11) is also shown in Fig. 1 by a short-dashed line. It is evident that the heating of the waveguide walls leads to enhanced laser pulse dissipation in comparison with the linear regime described by Eq. (11). The maximum temperature of the walls decreases with increasing distance as the pulse intensity becomes lower due to absorption in the walls. Figure 2 demonstrates the effect of the laser

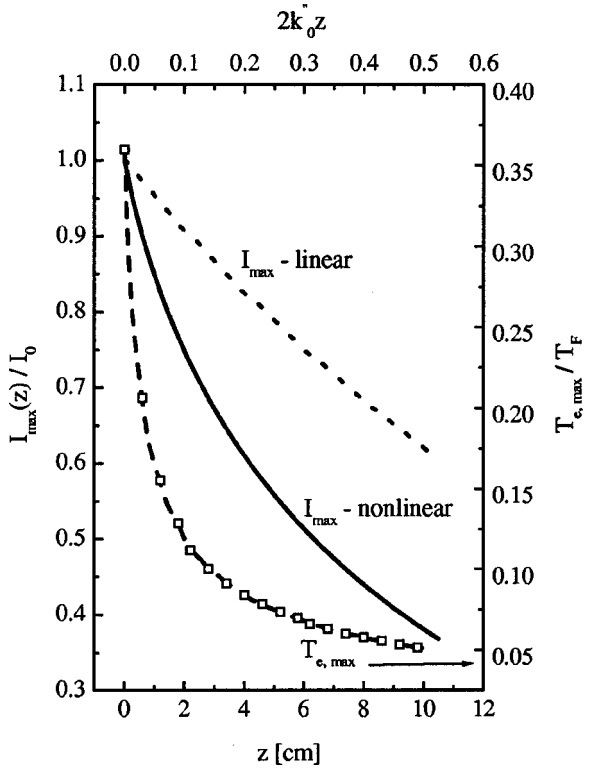

FIG. 1. The maximum values of the laser pulse intensity on the waveguide axis (solid line) and maximum electron temperature of the walls (line with squares) as functions of the distance of the laser pulse propagation in a Cu waveguide. For comparison, this intensity as computed by Eqs. (11) and (18) is given in the linear case (short-dashed line). Parameters are given in the text.

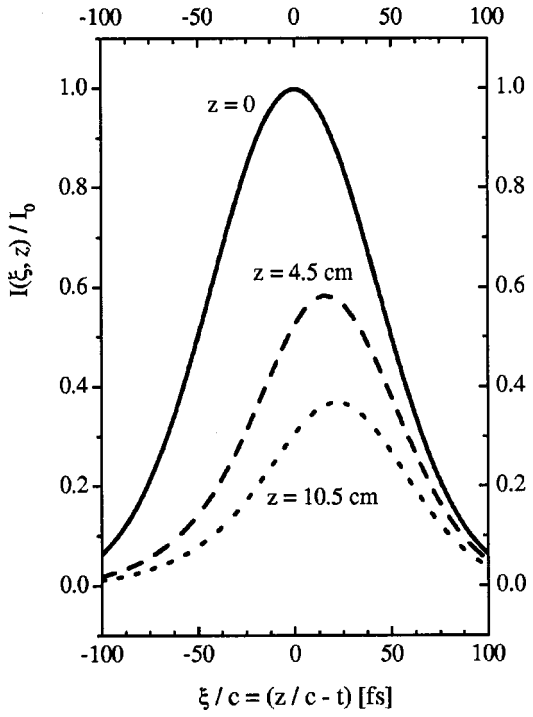

FIG. 2. The nonlinear modification of the temporal envelope of the laser pulse during propagation in a Cu waveguide for different values of the distance of propagation. $z=0$ cm, initial pulse, solid line; $z=4.5$ cm, dashed line; $z=10.5$ cm, short-dashed line. Parameters are the same as for Fig. 1 and are given in the text.

pulse shortening due to the wall heating in qualitative agreement with the simplified solution (37),(38).

In order to check that plasma formation at the metallic wall can be discarded, the absorbed laser flux at the metallic wall has to be less than the flux for which ablation and ionization take place for copper and for laser pulses of the same duration; this flux has been measured to be around 4×10^{12} W/cm^2 [18]. To get an estimation of the flux absorbed at the metallic wall at the maximum of the laser pulse, we use expression (32), with the maximum value of the temperature reached by the wall (after the maximum of the laser pulse) as it appears from Fig. 1, 2.8 eV; this gives an overestimated value of the absorbed flux of 3×10^{12} W/cm^2, less than the threshold for ablation and ionization.

Analogous results for an Al wave guide of the same width $2a=20\,\mu$m are presented in Figs. 3 and 4. In this case the parameters were $T_F=11$ eV, $\nu_0=1.25\times10^{14}$ s^{-1}, $\omega_p=2.32\times10^{16}$ s^{-1} [15], and the maximum initial laser pulse intensity was $I_0=0.75\times10^{15}$ W/cm^2. Concerning plasma formation, using the same arguments one finds that the absorbed flux at the Al wall is less than 8×10^{10} W/cm^2, well within the threshold for plasma formation.

As a consequence of the higher electron-phonon collision frequency ν_0 in Al, the laser pulse absorption is greater than in the Cu waveguide and is closer to the linear regime. Therefore the effect of pulse shortening is not so pronounced, as is seen from a comparison of Figs. 2 and 4.

V. DISCUSSION AND CONCLUSIONS

The propagation of a short intense laser pulse in a hollow metallic waveguide is accompanied by heating of the metallic walls. If the temperature of the electrons of the walls increases substantially within the laser pulse duration, the properties of the walls are changed and this nonlinear effect modifies the conditions of pulse propagation. In this paper we investigated the high frequency skin effect when the nonlinear effects are due to variations of the electron collision frequency in a metallic waveguide, therefore modifying the dissipation of the laser pulse energy into the walls.

The set of Eqs. (25)–(28), obtained together with Eq. (8) or Eq. (18) for TE or TM mode, respectively, describes self-consistently the heating of waveguide walls and the laser pulse propagation in the waveguide. The analytical and numerical analysis of these equations shows that the wall heating results in two points. First, the attenuation of the intense laser pulse increases in comparison with the linear regime, which is valid for weak laser pulses. Secondly, the temporal form of the laser pulse is changed in the process of pulse propagation. The energy of the leading part of the pulse decreases more slowly than that of the rear part, resulting in laser pulse shortening.

Our model of metallic waveguide walls is quantitatively correct in the case of a degenerate electron gas with the electron mean free path $l_e\cong V_F/\nu$ smaller than the skin depth $\delta\cong c/\omega_p$. These conditions imply the range of electron temperatures $T_F>T_e>T_{\min}$, where the lower limit is determined by the requirement $l_e<\delta$. For some metals such as lead and

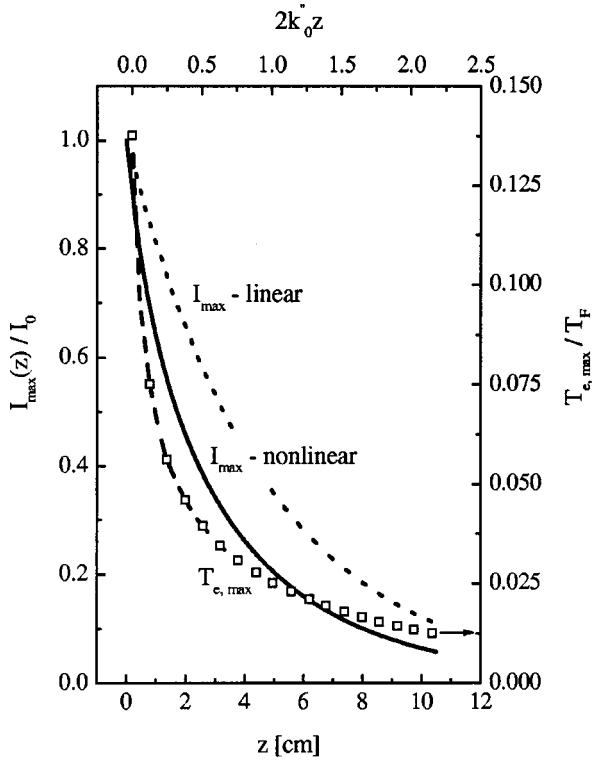

FIG. 3. The maximum values of the laser pulse intensity on the waveguide axis (solid line) and maximum electron temperature of the walls (line with squares) as functions of the distance of the laser pulse propagation in an Al waveguide. For comparison, this intensity as computed by Eqs. (11) and (18) is given in the linear case (short-dashed line). Parameters are given in the text.

magnesium, this condition is fulfilled at room temperature; but for metals such as copper and aluminum this requirement of sufficiently small electron mean free path is satisfied for $T_{\min} \geqslant T^* = (T_{\rm lat} T_F)^{1/2} \approx 0.5$ eV for typical parameters of metals ($T_F \approx 10$ eV, $T_{\rm lat} \approx 2.6 \times 10^{-2}$ eV$=300$ K). However, due to heating of the wall, the time during which the mean free path is longer than the skin depth is usually short compared to the pulse duration.

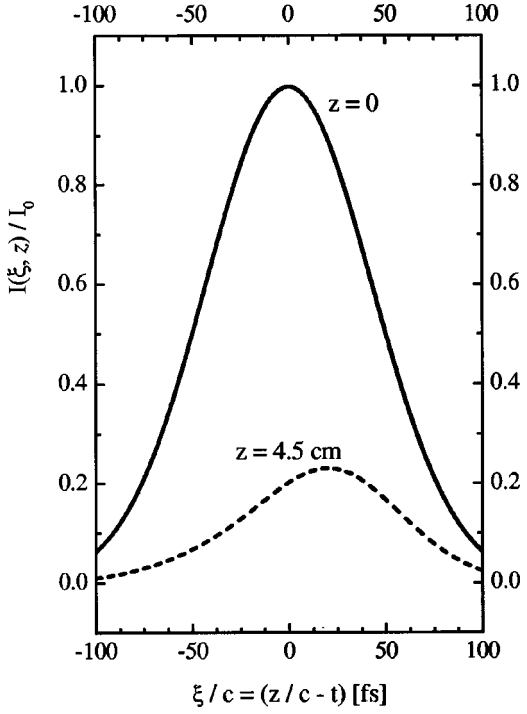

FIG. 4. The nonlinear modification of the temporal envelope of the laser pulse during propagation in an Al waveguide for different values of the distance of propagation. $z=0$ cm, initial pulse, solid line; $z=4.5$ cm, dashed line; $z=10.5$ cm, short-dashed line. Parameters are the same as for Fig. 1 and are given in the text.

The propagation of short laser pulses in waveguides where the walls have already been ionized will be the subject of a forthcoming paper.

The nonlinear phenomena discussed might be observed experimentally by measurements of the energy and temporal shape of the laser pulse transmitted through a metallic hollow waveguide provided that the linear damping does not depend on the roughness of the surface of the metallic wall.

ACKNOWLEDGMENT

This work was supported by INTAS Project No. 97-10236.

[1] G. Mourou, and D. Umstadter, Phys. Fluids B **4**, 2315 (1992).
[2] E. Esarey *et al.*, IEEE Trans. Plasma Sci. **24**, 252 (1996), and references therein.
[3] P. B. Corkum *et al.*, Phys. Rev. Lett. **62**, 1259 (1989).
[4] M. Tabak *et al.*, Phys. Plasmas **1**, 1626 (1994).
[5] T. Ditmire *et al.*, Nature (London) **386**, 54 (1997).
[6] A. B. Borisov *et al.*, Phys. Rev. A **45**, 5830 (1992).
[7] P. Sprangle and E. Esarey, Phys. Fluids B **4**, 2241 (1992).
[8] C. Dufree and H. Milchberg, Phys. Rev. Lett. **71**, 2409 (1993).
[9] A. Zigler *et al.*, J. Opt. Soc. Am. B **13**, 68 (1996).
[10] S. Jackel *et al.*, Opt. Lett. **20**, 1086 (1995).
[11] M. Borghesi *et al.*, Phys. Rev. E **57**, 4899 (1998).
[12] F. Dorchies *et al.*, Phys. Rev. Lett. **82**, 4655 (1999).
[13] E. A. J. Marcatili and R. A. Schmeltzer, Bell Syst. Tech. J., 1783 (1964).
[14] W. Rozmus *et al.*, Phys. Plasmas **3**, 360 (1996).
[15] N. W. Ashcroft, and N. D. Mermin, *Solid State Physics* (Holt, Rinehart and Winston, New York, 1976).
[16] A. Abrikosov, *Fundamentals of the Theory of Metals* (North-Holland, Amsterdam, 1988).
[17] A. P. Kanavin *et al.*, Phys. Plasmas **3**, 360 (1996).
[18] S. Nolte *et al.*, J. Opt. Soc. Am. B **14**, 2716 (1997).